

See discussions, stats, and author profiles for this publication at: <https://www.researchgate.net/publication/26782298>

Kinetic and Mechanistic Studies of Geometrical Isomerism in Neutral Square-Planar Methylpalladium Complexes Bearing Unsymmetrical Bidentate Ligands of α -Aminoaldimines

ARTICLE in INORGANIC CHEMISTRY · SEPTEMBER 2009

Impact Factor: 4.76 · DOI: 10.1021/ic900296y · Source: PubMed

CITATIONS

7

READS

31

9 AUTHORS, INCLUDING:



Mu-Chieh Chang

University of Groningen

13 PUBLICATIONS 70 CITATIONS

SEE PROFILE



Kuo-Hsuan Yu

National Taiwan University

7 PUBLICATIONS 59 CITATIONS

SEE PROFILE



Yu Wang

National Taiwan University

440 PUBLICATIONS 6,256 CITATIONS

SEE PROFILE



Shih-Tzung Liu

National Taiwan University

154 PUBLICATIONS 2,636 CITATIONS

SEE PROFILE

Kinetic and Mechanistic Studies of Geometrical Isomerism in Neutral Square-Planar Methylpalladium Complexes Bearing Unsymmetrical Bidentate Ligands of α -Aminoaldimines

Feng-Zhao Yang, Yu-Heng Wang, Mu-Chieh Chang, Kuo-Hsuan Yu, Shou-Ling Huang, Yi-Hung Liu, Yu Wang, Shih-Tzung Liu, and Jwu-Ting Chen*

Department of Chemistry, National Taiwan University, Taipei 106, Taiwan

Received February 13, 2009

A series of hemilabile ligands of α -aminoaldimines and their methylpalladium complexes have been prepared and characterized. Neutral square-planar methylpalladium complexes in the form of $[R^1R^2NCMe_2CH=NR]Pd(Me)Cl$ ($R=Me$, $R^1=R^2=Me$ (**3a**); $R=Me$, $R^1=Me$, $R^2=Et$ (**3b**); $R=Et$, $R^1=Me$, $R^2=Et$ (**4a**); $R=Et$, $R^1=Pr$, $R^2=Me$ (**5a**); $R=Pr$, $R^1=R^2=Me$ (**6a**); $R=Pr$, $R^1=R^2=Et$ (**6b**); $R=Pr$, (R^1, R^2)= C_4H_8 (**6c**); $R=Pr$, $R^1=Pr$, $R^2=H$ (**6d**); $R=Pr$, $R^1=^tBu$, $R^2=H$ (**6e**); $R=^tBu$, $R^1=R^2=Me$ (**7a**); $R=^tBu$, $R^1=Me$, $R^2=Et$ (**7b**); $R=^tBu$, (R^1, R^2)= C_4H_8 (**7c**); $R=^tBu$, $R^1=Pr$, $R^2=H$ (**7d**); $R=^tBu$, $R^1=^tBu$, $R^2=H$ (**7e**); $R=Ph$, $R^1=R^2=Me$ (**8a**); $R=Ph$, $R^1=Me$, $R^2=Et$ (**8b**)) show geometrical isomerism. The relative ratios of trans/cis isomers appear to be predominated by the steric hindrance between the Pd-bound methyl group and imino or amino substituents (R and R^1 and R^2). The NMR studies for the substitution reaction of $(COD)Pd(Me)Cl$ with $Et_2NCMe_2CH=N^iPr$ at $-20^\circ C$ indicate that *cis*-**6b** is the major kinetic product, which isomerizes to the thermodynamic product in trans form quantitatively above $-5^\circ C$. Kinetic results show that the ligand substitution reaction likely undergoes an associative pathway, and the isomerization reaction proceeds via an intramolecular process that comprises imine dissociation and recoordination.

Introduction

Square-planar coordination compounds with unsymmetrical bidentate ligands may carry the character of geometrical isomerism.¹ This property is worthy of investigation, because the structural differentiation in such isomerism potentially may convey distinct chemical reactivity.² The derivatives of α -aminoaldimines in the form of $R^1R^2NCMe_2CH=NR$ have been found to serve as hemilabile bidentate ligands of non- C_2 symmetry.³ These ligands bear

hybrid functionalities of amine and imine that possess nitrogen donors with sp^2 and sp^3 configuration, respectively. We previously found that these two functionalities appear to provide comparable trans influence. On the other hand, the amine and imine of α -aminoaldimines can have substituents with different numbers and varieties and thus can afford distinct steric influence on their vicinal ligands.⁴

In the cases of square-planar $[Et_2NCMe_2CH=NR]Pd(Me)Cl$ ($R = ^iPr$ (**6b**), Ph (**8b**)), the trans configuration that is defined according to the orientation of heavier donor

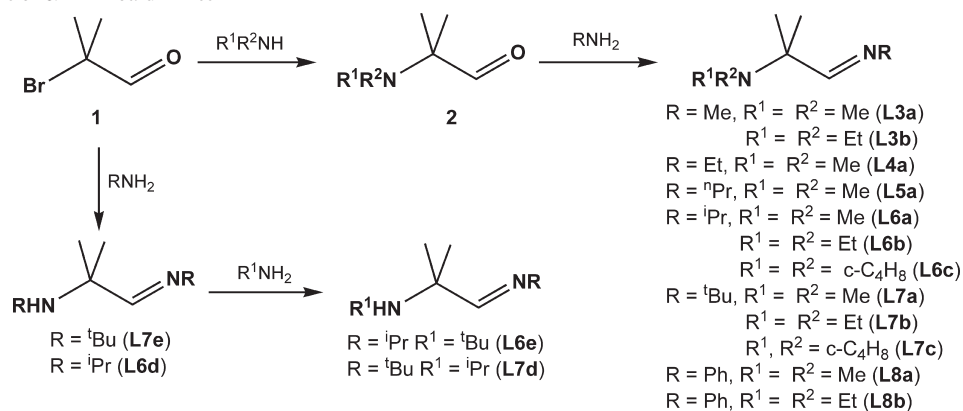
*To whom correspondence should be addressed. Tel.: 8862-3366-1659. Fax: 8862-2363-6359. E-mail: jtchen@ntu.edu.tw.

(1) (a) Rulke, R. E.; Delis, J. G. P.; Groot, A. M.; Elsevier, C. J.; van Leeuwen, P. W. N. M.; Vrieze, K.; Goubitz, K.; Schenk, H. *J. Organomet. Chem.* **1996**, 508, 109–120. (b) Nozaki, K.; Sato, N.; Tonomura, Y.; Yasutomi, M.; Takaya, H.; Hiyama, T.; Matsubara, T.; Koga, N. *J. Am. Chem. Soc.* **1997**, 119, 12779–12795. (c) Bastero, A.; Claver, C.; Ruiz, A.; Castillon, S.; Daura, E.; Bo, C.; Zangrando, E. *Chem.—Eur. J.* **2004**, 10, 3747–3760. (d) Soro, B.; Stoccoro, S.; Cinelli, M. A.; Minghetti, G.; Zucca, A.; Bastero, A.; Claver, C. *J. Organomet. Chem.* **2004**, 689, 1521–1529. (e) Owen, G. R.; Burkill, H. A.; Vilar, R.; White, A. J. P.; Williams, D. J. *J. Organomet. Chem.* **2005**, 690, 5113–5124. (f) Centore, R.; Roviello, G.; Tuzi, A. *Inorg. Chim. Acta* **2005**, 358, 2112–2116. (g) Amenta, D. S.; Sparks, S. N.; Giljea, J. W.; Edelman, F. T.; Fischer, A.; Blaurock, S. Z. *Inorg. Allg. Chem.* **2005**, 631, 2854–2857. (h) Durand, J.; Zangrando, E.; Stener, M.; Fronzoni, G.; Carfagna, C.; Binotti, B.; Kamer, P. C. J.; Muller, C.; Caporali, M.; van Leeuwen, P. W. N. M.; Vigt, D.; Milani, B. *Chem.—Eur. J.* **2006**, 12, 7639–7651. (i) Braunstein, P. *Chem. Rev.* **2006**, 106, 134–159. (j) Vuzman, D.; Poverenov, E.; Shimon, L. J. W.; Diskin-Posner, Y.; Milstein, D. *Organometallics* **2008**, 27, 2627–2634.

(2) (a) van Leeuwen, P. W. N. M.; Roobeek, C. F.; van der Heijden, H. *J. Am. Chem. Soc.* **1994**, 116, 12117–12118. (b) Hamilton, D. H.; Shapley, J. R. *Organometallics* **1998**, 17, 3087–3090. (c) Ding, Y.; Fanwick, P. E.; Walton, R. A. *Inorg. Chem.* **1999**, 38, 5165–5170. (d) Clarkson, A. J.; Blackman, A. G.; Clark, C. R. *J. Chem. Soc., Dalton Trans.* **2001**, 758–765. (e) Vicente, J.; Abad, J.-A.; Martínez-Viviente, E. *Organometallics* **2002**, 21, 4454–4467. (f) Vicente, J.; Abad, J.-A.; Förtsch, W.; López-Sáez, M.-J. *Organometallics* **2004**, 23, 4414–4429. (g) Madej, E.; Katafias, A.; Kita, P.; Eriksen, J.; Mønsted, O. *Eur. J. Inorg. Chem.* **2006**, 5098–5105. (h) Huynh, H. V.; Ho, J. H. H.; Neo, T. C.; Koh, L. L. *J. Organomet. Chem.* **2005**, 690, 3854–3860. (i) Carfagna, C.; Gatti, G.; Mosca, L.; Paoli, P.; Guerri, A. *Helv. Chim. Acta* **2006**, 89, 1660–1671. (j) Leone, A.; Gischig, S.; Elsevier, C. J.; Consiglio, G. *J. Organomet. Chem.* **2007**, 692, 2056–2063. (k) Casares, J. A.; Espinet, P.; Martínez-Illarduya, J. M.; Mucientes, J. J.; Salas, G. *Inorg. Chem.* **2007**, 46, 1027–1032.

(3) Lee, J.-J.; Yang, F.-Z.; Lin, Y.-F.; Chang, Y.-C.; Yu, K.-H.; Chang, M.-C.; Lee, G.-H.; Liu, Y.-H.; Wang, Y.; Liu, S.-T.; Chen, J.-T. *Dalton Trans.* **2008**, 5945–5956.

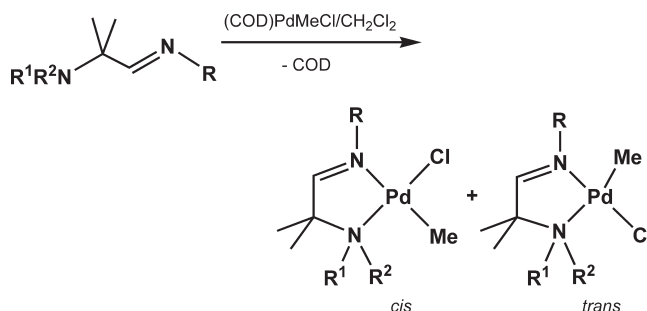
(4) Yang, F.-Z.; Chen, Y.-C.; Lin, Y.-F.; Yu, K.-H.; Liu, Y.-H.; Wang, Y.; Liu, S.-T.; Chen, J.-T. *Dalton Trans.* **2009**, 1243–1250.

Scheme 1. Synthesis of α -Aminoaldimines

atoms of Cl and N(sp²) toward the metal center has been found to be the sole isomer.³ DFT calculations for the geometrical isomers gave energy preferences of -17.1 kJ/mol for *trans*-**6b** and -20.8 kJ/mol for *trans*-**8b** to their *cis* analogues. The favored stability of the *trans* form is attributed to the methyl ligand's inclination to being seated at the site *cis* to imine, for which the Pd–N(sp²)–R angles (generally $> 120^\circ$) can undertake more steric tolerance than the Pd–N(sp³)–R angles in amines (generally $< 110^\circ$). The theme of this study details our further investigation along the line by varying amino and imino substituents of α -aminoaldimine ligands in the square-planar chloromethylpalladium complexes, which can fine-tune the geometrical isomerism. The kinetics and mechanism of isomerization and formation reactions of $[\text{Et}_2\text{NCMe}_2\text{CH=NR}]\text{Pd}(\text{Me})\text{Cl}$ have also been examined.

Results and Discussion

1. Synthesis and Structures. The synthesis of α -aminoaldimine in the form of $\text{R}^1\text{R}^2\text{NCMe}_2\text{CH=NR}$ has succeeded, as illustrated in Scheme 1. Substitution of a secondary amine for bromine in 2,2-bromomethylpropanal (**1**) gives 2,2-aminomethylpropanal (**2**).⁵ Successive condensation reactions between **2** and a primary amine afford the desired products ($R = \text{Me}, R^1 = R^2 = \text{Me}$ (**L3a**); $R = \text{Me}, R^1 = R^2 = \text{Et}$ (**L3b**); $R = \text{Et}, R^1 = R^2 = \text{Me}$ (**L4a**); $R = n\text{Pr}, R^1 = R^2 = \text{Me}$ (**L5a**); $R = i\text{Pr}, R^1 = R^2 = \text{Me}$ (**L6a**); $R = i\text{Pr}, R^1 = R^2 = \text{Et}$ (**L6b**); $R = i\text{Pr}, (R^1, R^2) = c\text{-C}_4\text{H}_8$ (**L6c**); $R = t\text{Bu}, R^1 = R^2 = \text{Me}$ (**L7a**); $R = t\text{Bu}, R^1 = R^2 = \text{Et}$ (**L7b**); $R = t\text{Bu}, (R^1, R^2) = c\text{-C}_4\text{H}_8$ (**L7c**); $R = \text{Ph}, R^1 = R^2 = \text{Me}$ (**8a**), $R = \text{Ph}, R^1 = R^2 = \text{Et}$ (**8b**)). When *iso*-propylamine or *tert*-butylamine reacts with **1**, substitution and condensation may be achieved in a one-pot reaction. As a consequence, α -aminoaldimines in the form of $\text{RHNMe}_2\text{CH=NR}$ ($R = i\text{Pr}$ (**L6d**), $t\text{Bu}$ (**L7e**)) could be prepared. Using an excess of *iso*-propylamine with **L7e** or *tert*-butylamine with **L6d**, the imino substituent could be replaced, affording $\text{R}^1\text{HNCMe}_2\text{CH=NR}$ ($R = i\text{Pr}, R^1 = t\text{Bu}$ (**L6e**); $R = t\text{Bu}, R^1 = i\text{Pr}$ (**L7d**)) in fair

Scheme 2. Formation of $[\text{R}^1\text{R}^2\text{NCMe}_2\text{CH=NR}]\text{Pd}(\text{Me})\text{Cl}$ 

yields. All products were purified by distillation and characterized mainly by NMR techniques.

The neutral organometallic complexes in the form of $[\text{R}^1\text{R}^2\text{NCMe}_2\text{CH=NR}]\text{Pd}(\text{Me})\text{Cl}$ ($R = \text{Me}, R^1 = R^2 = \text{Me}$ (**3a**); $R = \text{Me}, R^1 = R^2 = \text{Et}$ (**3b**); $R = \text{Et}, R^1 = R^2 = \text{Me}$ (**4a**); $R = n\text{Pr}, R^1 = R^2 = \text{Me}$ (**5a**); $R = i\text{Pr}, R^1 = R^2 = \text{Me}$ (**6a**); $R = i\text{Pr}, R^1 = R^2 = \text{Et}$ (**6b**); $R = i\text{Pr}, (R^1, R^2) = c\text{-C}_4\text{H}_8$ (**6c**); $R = i\text{Pr}, R^1 = i\text{Pr}, R^2 = \text{H}$ (**6d**); $R = i\text{Pr}, R^1 = t\text{Bu}, R^2 = \text{H}$ (**6e**); $R = t\text{Bu}, R^1 = R^2 = \text{Me}$ (**7a**); $R = t\text{Bu}, R^1 = R^2 = \text{Et}$ (**7b**); $R = t\text{Bu}, (R^1, R^2) = c\text{-C}_4\text{H}_8$ (**7c**); $R = t\text{Bu}, R^1 = i\text{Pr}, R^2 = \text{H}$ (**7d**); $R = t\text{Bu}, R^1 = t\text{Bu}, R^2 = \text{H}$ (**7e**); $R = \text{Ph}, R^1 = R^2 = \text{Me}$ (**8a**), $R = \text{Ph}, R^1 = R^2 = \text{Et}$ (**8b**)) could be readily prepared via substitution of α -aminoaldimine for COD (1,5-cyclooctadiene) in $(\text{COD})\text{Pd}(\text{Me})\text{Cl}$ (Scheme 2).⁶

The single crystals of *trans*-**6d**, *trans*-**6e**, *cis*-**7d**, and *trans*-**8a** were grown from $\text{CH}_2\text{Cl}_2/n\text{-hexane}$. The crystal data and selected bond parameters are collected in the Tables S4 and S5 (Supporting Information). The representative ORTEP drawings of *trans*-**6e** and *cis*-**7d** with thermal ellipsoids at 30% probability are shown in Figure 1. The four-coordinate molecular structures in square-planar geometry are confirmed. In the complexes of the *trans* form, the bond distances of Pd–N(sp²), Pd–N(sp³), Pd–C, and Pd–Cl as well as the bite angles of N(sp²)–Pd–N(sp³) and C–Pd–Cl are quite comparable to those of known chloromethylpalladium analogues *trans*-**6b** and *trans*-**8b**.³ The noticeable difference is that the angles of C5–N2–Pd in **6d** and **6e** are substantially larger ($5\text{--}7^\circ$) than in **6b** and **8b**. This is presumably due to

(5) (a) Fisher, L. E.; Muchowski, J. M. *Org. Prep. Proced. Int.* **1990**, 22, 399. (b) Sibi, M. P.; Zhang, R.; Manyem, S. J. *Am. Chem. Soc.* **2003**, 125, 9306–9307. (c) Sibi, M. P.; Stanley, L. M. *Tetrahedron: Asymmetry* **2004**, 15, 3353–3356. (d) Larionov, S. V.; Tkachev, A. V.; Savel'eva, Z. A.; Myachina, L. I.; Glinskaya, L. A.; Klevtsova, R. F.; Bizyaev, S. N. *Russ. J. Coord. Chem.* **2006**, 32, 250–260.

(6) (a) Stoccoro, S.; Minghetti, G.; Cinellu, M. A.; Zucca, A.; Manassero, M. *Organometallics* **2001**, 20, 4111–4113. (b) Liu, W.; Brookhart, M. *Organometallics* **2004**, 23, 6099–6107. (c) Wang, R.; Twamley, B.; Shreeve, J. M. *J. Org. Chem.* **2006**, 71, 426–429.

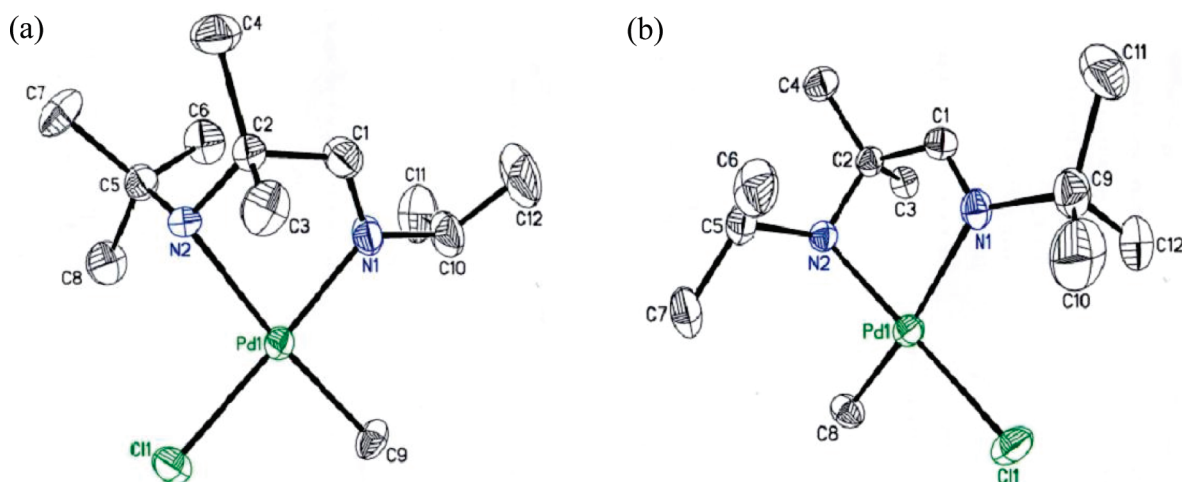


Figure 1. ORTEP drawing of (a) *trans*-**6e** and (b) *cis*-**7d**. All hydrogen atoms are omitted for clarity.

the steric hindrance among the amino substituents in the secondary amine possibly being substantially smaller than that in tertiary amine.

Contrary to all *trans* analogues, the distance of Pd–N(sp²) in *cis*-**7d** is 0.11 Å longer than that of Pd–N(sp³). This surprising result suggests that the geometrical configuration is a major factor affecting the bonding rather than atomic hybridization. This gives further evidence of that imino- and amino-nitrogen atoms are not very different in electronic contribution to the coordination with the metal.³ As a consequence, α-aminoaldimines may serve the C₂-unsymmetrical bidentate auxiliary ligands with predominant coordinating differentiation in steric control.

2. Geometrical Isomerism. The ¹H NMR spectra clearly indicate that there are two geometrical isomers for the chloromethylpalladium complexes bearing α-aminoaldimines in most cases of this study. The nuclear Overhauser effect spectrometry technique provides the unequivocal assignment for the isomers. The Pd-bound methyl signals corresponding to the *cis* isomers are located in the range of δ 0.5–0.7 and are of higher field than those corresponding to their *trans* form (δ 0.6–0.8). Thus, they serve as effective and convenient probes for the identification of these isomers.⁷

The relative ratios for the isomers could be readily measured by NMR integrations. The percentage ratios of *trans* complexes **3**–**7** are listed in Table 1. At 22 °C, the relative ratios for the *trans* forms of **3a**, **3b**, **4a**, **5a**, **6a**, and **6b** are quite comparable and show little dependence on

Table 1. Percentage Ratio of *trans* Isomers

| complex | R | R ¹ | R ² | rel. ratio ^a (<i>trans</i> %) | K |
|------------------------|-----------------|-----------------------------------------|----------------|-------------------------------------------|-------|
| 3a | Me | Me | Me | 97 | 32 |
| 3b | Me | Et | Et | ≥99 | |
| 4a | Et | Me | Me | ≥99 | |
| 5a | ⁱ Pr | Me | Me | ≥99 | 13 |
| 6a | ⁱ Pr | Me | Me | 93 | |
| 6b | ⁱ Pr | Et | Et | ≥99 | |
| 6c | ⁱ Pr | <i>c</i> -C ₄ H ₈ | | 95 | 19 |
| 6d | ⁱ Pr | ⁱ Pr | H | 54 | |
| 6e | ⁱ Pr | ⁱ Bu | H | 78 | |
| 7a | ⁱ Bu | Me | Me | 15 | 0.18 |
| 7b | ⁱ Bu | Et | Et | 60 | |
| 7c | ⁱ Bu | <i>c</i> -C ₄ H ₈ | | 34 | |
| 7d | ⁱ Bu | ⁱ Pr | H | 5.0 | 0.053 |
| 7e | ⁱ Bu | ⁱ Bu | H | 12 | |
| 8a | Ph | Me | Me | ≥99 | |
| 8b ³ | Ph | Et | Et | ≥99 | 0.14 |

^aThe percentage ratios were measured by ¹H NMR integrations in CDCl₃.

the amino substituents. One may conclude that, in such a square-planar complex, the methyl or ethyl substituent on the imino group gives indistinguishable hindrance to the adjacent methyl ligand. For **6d** and **6e**, secondary amines can substantially stabilize the *cis* isomers, when the imino substituent is an isopropyl group.

The *trans* abundance shows remarkable depletion for derivatives **7** in which the imino substituent is a bulky tertiary butyl group. It appears that the *cis* configuration of studied complexes may be favored when the imino substituent becomes sufficiently bulky. In addition, the geometrical isomerism becomes susceptible to variation of the amino substituents. When the relative ratios of the isomers for the complexes **7** are viewed, the *cis* derivatives are predominant, when the amino moiety is of the secondary class, as in **7d** and **7e**. When **7b** is compared with **7a**, in which the two amino substituents are ethyl and methyl, respectively, the *trans* percentage drops from 60 to 15. Between **7b** and **7c**, the amino substituents have the same composition of C₄H₈, but in distinct acyclic and cyclic skeletons. The *trans* percentages are 66 and 33, respectively.

Such results are attributed to the competition in releasing steric hindrances between Pd-bound methyl and the

(7) (a) Nozaki, K.; Hiyama, T. *Organometallics* **2000**, *19*, 2031–2035. (b) Coleman, K. S.; Green, M. L. H.; Pascu, S. I.; Rees, N. H.; Cowley, A. R.; Rees, L. H. *Dalton Trans.* **2001**, 3384–3395. (c) Dahan, F.; Dyer, P. W.; Hanton, M. J.; Jones, M.; Mingos, D. M. P.; White, A. J. P.; Williams, D. J.; Williamson, A.-M. *Eur. J. Inorg. Chem.* **2002**, 732–742. (d) Froese, M.; Dhindsa, A.; Roise, H.; Tilset, M. *Dalton Trans.* **2003**, 4516–4524. (e) Groux, L. F.; Weiss, T.; Reddy, D. N.; Chase, P. A.; Piers, W. E.; Ziegler, T.; Parvez, M.; Benet-Buchholz, J. J. *Am. Chem. Soc.* **2005**, *127*, 1854–1869. (f) Anderson, C. E.; Apperley, D. C.; Batsanov, A. S.; Dyer, P. W.; Howard, J. A. K. *Dalton Trans.* **2006**, 4134–4145. (g) Carfagna, C.; Gatti, G.; Mosca, L.; Paoli, P.; Guerri, A. *Helv. Chim. Acta* **2006**, *89*, 1660–1671. (h) Canovesi, L.; Visentin, F.; Santo, C.; Levi, C.; Dolmella, A. *Organometallics* **2007**, *26*, 5590–5601. (i) Ceder, R. M.; Muller, G.; Ordinas, M.; Ordinas, J. I. *Dalton Trans.* **2007**, 83–90. (j) Bella, A. F.; Ruiz, A.; Claver, C.; Sepulveda, F.; Jalon, F. A.; Manzano, B. R. *J. Organomet. Chem.* **2008**, *693*, 1269–1275.

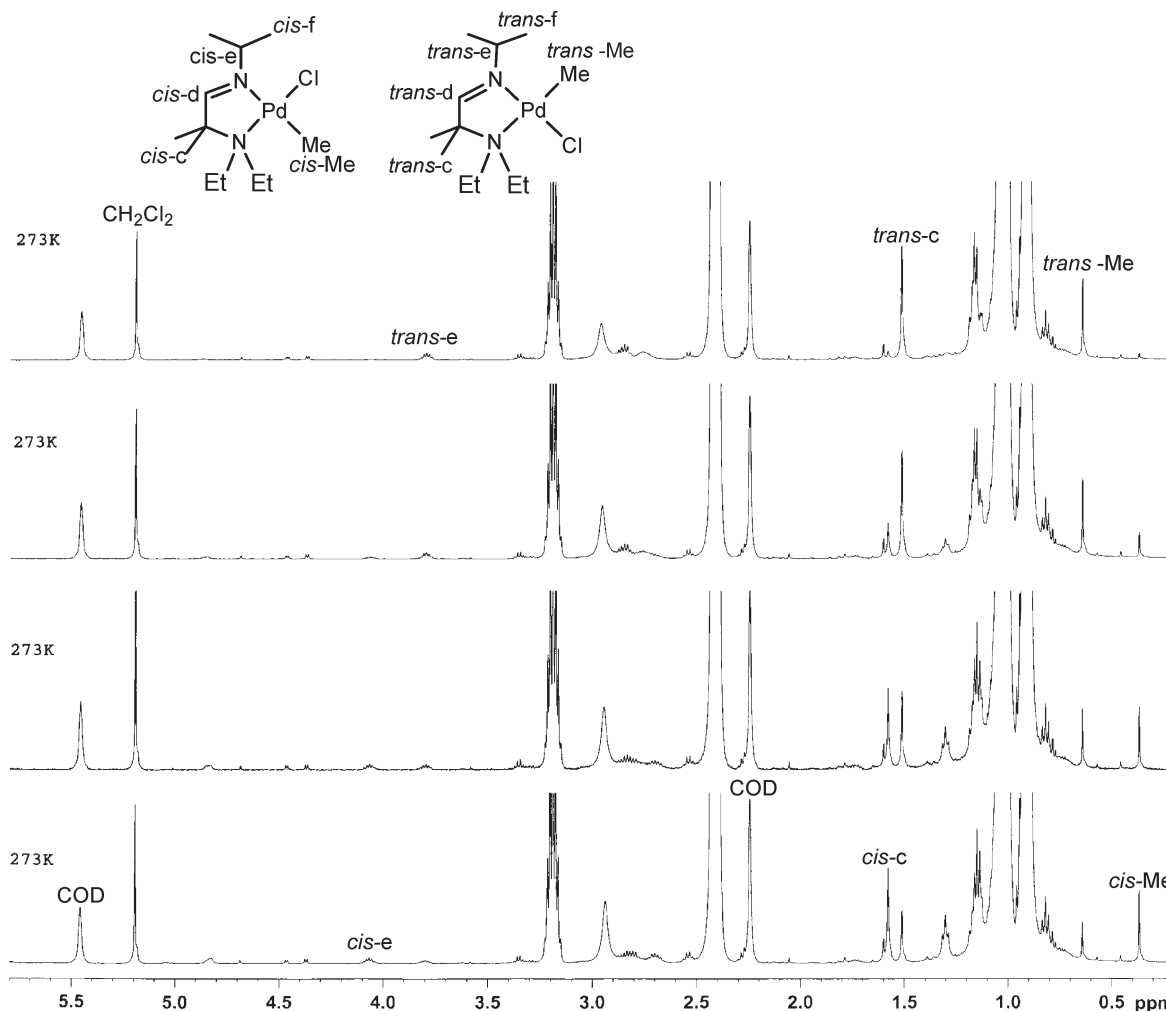
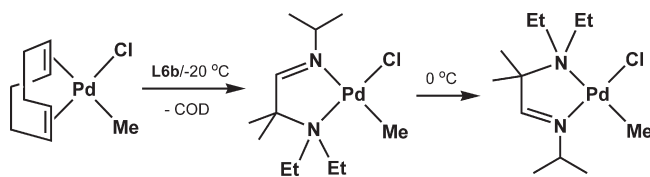


Figure 2. Time-resolved ^1H NMR spectra for the reaction of $(\text{COD})\text{Pd}(\text{Me})\text{Cl}$ and **L6b** at 0°C in CDCl_3 .

Scheme 3. Kinetic and Thermodynamic Products of the Reaction of $(\text{COD})\text{Pd}(\text{Me})\text{Cl}$ with $\text{Et}_2\text{NCMe}_2\text{CH}=\text{N}^i\text{Pr}$ (**L6b**)



substituents of imine or amine. When the substituent on imine is small, the methyl favors being *cis* to imine, because of the more spacial vicinity around the sp^2 nitrogen compared to the sp^3 nitrogen. When the imine substituent is sufficiently large, the methyl ligand might compromise by seating at the site *cis* to amine. The amino substituents will get a chance to affect the methyl ligand and thus can fine-tune the geometrical isomerism.^{1b,1c,8} This is consistent with the aforementioned structural results.

3. Kinetics and Mechanisms. In order to understand the mechanism of the isomerization reactions of these methylpalladium complexes with α -aminoaldimines, the reactions of $(\text{COD})\text{Pd}(\text{Me})\text{Cl}$ with α -aminoaldimines

were investigated by NMR at varied temperatures.^{1d,6b,9} In the case of **6b**, the mixtures of $(\text{COD})\text{Pd}(\text{Me})\text{Cl}$ (14.6 mg, 0.056 mmol) and **L6b** (47.5 mg, 0.258 mmol) were dissolved in 0.5 mL of CDCl_3 at -30°C and monitored. At -20°C , *cis*-**6b** was first observed as the major product. When the temperature was raised to -5°C , the isomerization from *cis* to *trans* could be monitored. At 25°C , *trans*-**6b** accounts for the sole thermodynamic product of substitution in quantitative yield (Scheme 3). In the analogous experiment of **L8b**, no other isomer could ever been observed besides *trans*-**8b**. In other cases such as **L7a**, **L7b**, **L7c**, and **L7e**, the substitution reactions result in geometrical isomerism to a varied extent.

Figure 2 displays a time-resolved ^1H NMR study for the reaction of $(\text{COD})\text{Pd}(\text{Me})\text{Cl}$ and **L6b** at 0.0°C . The spectral change clearly demonstrates the transformation of *cis*-**6b** to *trans*-**6b**. The geometrical isomerization of **6b** was monitored by measuring the signals with respect to $\text{Pd}-\text{CH}_3$ results for the first-order kinetics, as illustrated in

(8) (a) Elguero, J.; Guerrero, A.; de la Torre, F. G.; de la Hoz, A.; Jalon, F. A.; Manzano, B. R.; Rodriguez, A. *New J. Chem.* **2001**, 25, 1050–1060. (b) Leone, A.; Consiglio, G. *J. Organomet. Chem.* **2006**, 691, 4204–4214.

(9) Rülke, R. E.; Kaasjager, V. E.; Kliphuis, D.; Elsevier, C. J.; van Leeuwen, P. W. N. M.; Vrieze, K. *Organometallics* **1996**, 15, 668–677. (b) Setsune, J.-i.; Yamauchi, T.; Tanikawa, S.; Hirose, Y.; Watanabe, J.-y. *Organometallics* **2004**, 23, 6058–6065. (c) Groen, J. H.; Vlaar, M. J. M.; van Leeuwen, P. W. N. M.; Vrieze, K.; Kooijman, H.; Spek, A. L. *J. Organomet. Chem.* **1998**, 551, 67–79.

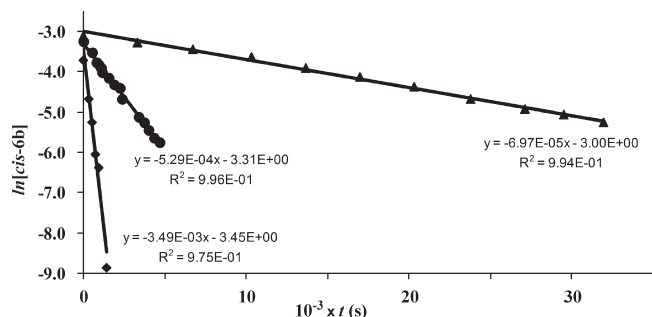


Figure 3. First-order kinetic plots for the isomerization reaction of **6b** in CDCl_3 (▲, -10°C ; ●, 0°C ; ◆, 10°C).

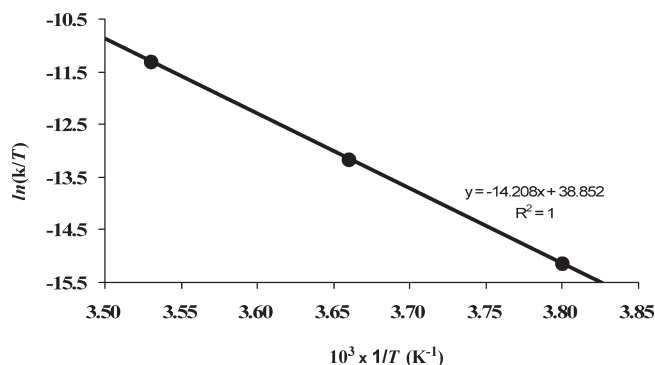


Figure 4. Eyring relationship for the isomerization reaction of **6b** in CDCl_3 .

Figure 3. The rate constants k_{isom} could be evaluated as $7.0 \times 10^{-5} \text{ s}^{-1}$ at -10°C , $5.3 \times 10^{-4} \text{ s}^{-1}$ at 0°C , and $3.5 \times 10^{-3} \text{ s}^{-1}$ at 10°C . The linear Eyring plot, as shown in Figure 4, provides the estimation for the enthalpy of activation ($\Delta H_{\text{isom}}^\ddagger$) as 118 kJ/mol and the entropy of activation ($\Delta S_{\text{isom}}^\ddagger$) as 126 J/mol K. At 0°C , the k_{isom} 's for **6a** and **3b** were evaluated similarly as $5.5 \times 10^{-4} \text{ s}^{-1}$ and $1.4 \times 10^{-3} \text{ s}^{-1}$, respectively (Figure S1, Supporting Information), indicating that isomerization is dependent on the imine substituent. The positive value of $\Delta S_{\text{isom}}^\ddagger$ suggests that the isomerization reactions likely undergo dissociative activation. Accordingly, the geometrical isomerization is proposed to proceed via a mechanism of imine dissociation and recoordination, as illustrated in Scheme 4. Such isomerization reactions in other analogous derivatives appear not as clear as these studied cases, even at -50°C . Another similar pathway through dissociative activation of the amine might not be excluded.

Kinetic studies for the substitution reactions of $(\text{COD})\text{Pd}(\text{Me})\text{Cl}$ with **L6a**, **L6b**, **L7a**, **L7c**, and **L8b** were also done in CDCl_3 by recording the ^1H NMR integration for the COD signals corresponding to $(\text{COD})\text{Pd}(\text{Me})\text{Cl}$ versus the reaction time. In a typical run, the mixture of $(\text{COD})\text{Pd}(\text{Me})\text{Cl}$ (6.0 mg, 0.0134 mmol) and **L8b** (74 mg, 0.34 mmol) was dissolved in 0.50 mL of thermostatted CDCl_3 . The ^1H NMR spectra were recorded with suitable intervals for more than three half-lives. The disappearance of $(\text{COD})\text{Pd}(\text{Me})\text{Cl}$ follows the first-order kinetics. The linear kinetic plots corresponding to the reactions of $(\text{COD})\text{Pd}(\text{Me})\text{Cl}$ with **L6a**, **L6b**, **L7a**, **L7c**, and **L8b** at 0°C , as shown in Figure 5, give the values of k_{obsd} . Using the rate law, $k_{\text{obsd}} = k[\text{L}]$, the second-order rate constants

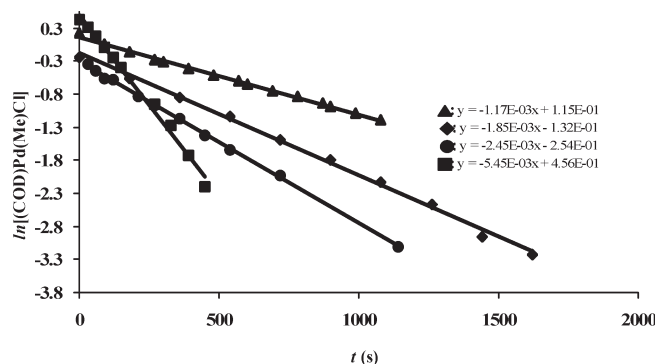


Figure 5. Pseudo-first-order kinetic plots for the substitution reactions of $(\text{COD})\text{Pd}(\text{Me})\text{Cl}$ with various α -aminoaldehydes at 0°C in CDCl_3 (◆, **L6a**; ■, **L6b**; ●, **L7a**; ▲, **L7c**).

k could be evaluated. The evaluation for thermodynamic parameters of activation was done according to Eyring relationships. The data for k_{obsd} and k_{subs} as well as $\Delta H_{\text{subs}}^\ddagger$, $\Delta S_{\text{subs}}^\ddagger$, and $\Delta G_{\text{subs}}^\ddagger$ corresponding to k_{subs} are collected in Table 2.

The negative values of $\Delta S_{\text{subs}}^\ddagger$, although small, implicate that the substitution reactions likely undergo an associative (or intermediate associative) pathway. A mechanism for the formation of $[\text{R}^1\text{R}^2\text{NCMe}_2\text{CH}=\text{NR}]\text{Pd}(\text{Me})\text{Cl}$ via ligand substitution from $(\text{COD})\text{Pd}(\text{Me})\text{Cl}$ is also summarized in Scheme 4, in which the α -aminoaldehyde is considered to first attach the metal of $(\text{COD})\text{Pd}(\text{Me})\text{Cl}$.

Looking into the thermodynamic data in Table 2, the significant differences of $\Delta G_{\text{subs}}^\ddagger$ between **L6a** and **L7a** and between **L6b** and **L8b** show the dependence on imino substituents. In addition, the bulkier *t*-butyl on imine results in a larger $\Delta G_{\text{subs}}^\ddagger$ than does isopropyl. On the other hand, the reactions for **L7a** and **L7c** show comparable values of $\Delta G_{\text{subs}}^\ddagger$. However, the difference of $\Delta G_{\text{subs}}^\ddagger$ values between the reactions for **L6a** and **L6b** is relatively large. Recalling the kinetic products of the *cis* configuration, the imine is *trans* to the methyl ligand, which is of strong *trans* effect. A pathway with imine as the entering functionality may be favored (Scheme 4). A similar pathway with the amine side as the entering functionality should not be excluded. The NMR measuring difficulty has limited experimental flooding conditions; the backward reactions and the possibility of a solvent dependence thus are overlooked in the studied cases.

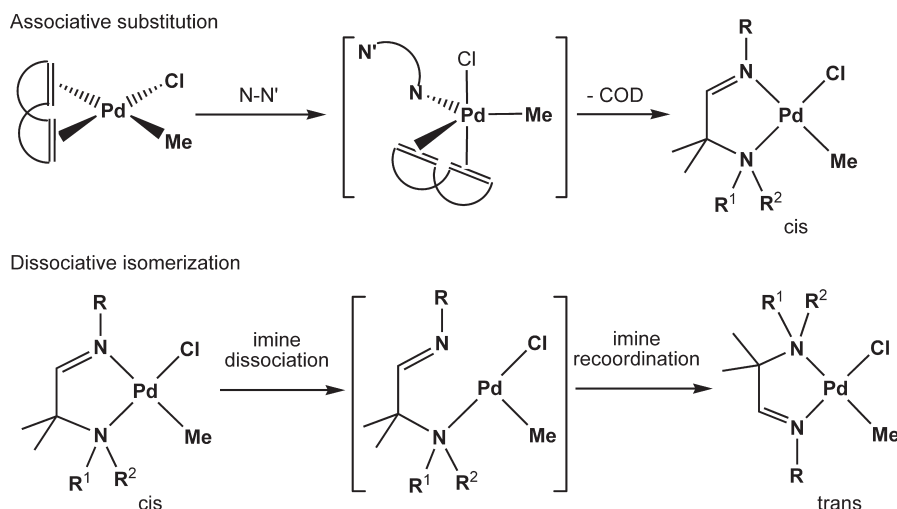
Such α -aminoaldehyde ligands allow the equipping of a coordination of bidentate chelation with functionally different but electronically comparable donors and sterically distinguishable environments around the metal. The fine-tuned geometrical isomerism in $[\text{R}^1\text{R}^2\text{NCMe}_2\text{CH}=\text{NR}]\text{Pd}(\text{Me})\text{Cl}$ of square-planar configuration simply by changing amino and imino substituents is a good illustration of an unsymmetrical bidentate ligand being able to result in fundamental selectivity of the coordination.

Experimental Section

General Procedures. Commercially available reagents were purchased and used without further purification unless otherwise indicated. Toluene, hexane, and diethyl ether were distilled from purple solutions of sodium benzophenone ketyl under nitrogen, and dichloromethane was dried over P_2O_5 and

Table 2. Kinetic Data for the Substitution Reactions of (COD)Pd(Me)Cl with α -Aminoaldehydes in CDCl₃

| | $k_{\text{subs}} (-5\text{ }^{\circ}\text{C}) (\text{M}^{-1} \text{s}^{-1})$ | $k_{\text{subs}} (0\text{ }^{\circ}\text{C}) (\text{M}^{-1} \text{s}^{-1})$ | $k_{\text{subs}} (5\text{ }^{\circ}\text{C}) (\text{M}^{-1} \text{s}^{-1})$ | $k_{\text{subs}} (10\text{ }^{\circ}\text{C}) (\text{M}^{-1} \text{s}^{-1})$ | $k_{\text{subs}} (15\text{ }^{\circ}\text{C}) (\text{M}^{-1} \text{s}^{-1})$ | $\Delta H_{\text{subs}}^{\ddagger} (\text{kJ/mol})$ | $\Delta S_{\text{subs}}^{\ddagger} (\text{J/mol K})$ | $\Delta G_{\text{subs}}^{\ddagger} (\text{kJ/mol})$ |
|------------|------------------------------------------------------------------------------|-----------------------------------------------------------------------------|-----------------------------------------------------------------------------|------------------------------------------------------------------------------|------------------------------------------------------------------------------|-----------------------------------------------------|------------------------------------------------------|-----------------------------------------------------|
| L6a | | 1.57×10^{-2} | 1.9×10^{-2} | 3.04×10^{-2} | 5.21×10^{-2} | 50.4 | -14.5 | 52.7 |
| L6b | 9.2×10^{-4} | 2.18×10^{-3} | 3.38×10^{-3} | 6.05×10^{-3} | | 75.5 | -5.45 | 77.7 |
| L7a | | 3.22×10^{-3} | 5.32×10^{-3} | 8.85×10^{-3} | 2.12×10^{-2} | 78.0 | -3.86 | 80.3 |
| L7c | | 1.95×10^{-3} | 4.03×10^{-3} | 7.68×10^{-3} | 1.19×10^{-2} | 77.3 | -4.56 | 79.4 |
| L8b | 3.90×10^{-3} | 7.4×10^{-3} | 1.12×10^{-2} | 1.76×10^{-2} | | 60.0 | -10.9 | 62.3 |

Scheme 4. Mechanism of Formation and Isomerization of $[\text{R}^1\text{R}^2\text{NCMe}_2\text{CH=NR}]\text{Pd}(\text{Me})\text{Cl}$ 

distilled immediately prior to use. Air-sensitive material was manipulated under a nitrogen atmosphere in a glovebox or by standard Schlenk techniques. The IR spectra were recorded on a Bio-Rad FTS-40 spectrophotometer. The NMR spectra were measured on a Bruker AC-300, AC-400, or AC-500 spectrometer. The corresponding frequencies for ^{13}C NMR spectra were 75.469, 100.625, or 125.753 MHz, respectively. Values upfield of ^1H and ^{13}C data are given in δ (ppm) relative to tetramethylsilane (δ 0.00) in CDCl₃. All spectra were obtained at ambient temperature unless stated otherwise. Mass spectrometric analyses were collected on a JEOL SX-102A or WATERS LCT Premier XE spectrometer. Elemental analysis was done on a Perkin-Elmer 2400 CHN analyzer. Details for the synthesis of the ligands and complexes are given in the Supporting Information.

Kinetic Study. Kinetic measurements for the reactions of (COD)Pd(Me)Cl and **L6a**, **L6b**, **L7a**, and **L8b** were done under pseudo-first-order conditions. In a typical run, the mixtures of (COD)Pd(Me)Cl (6.0 mg, 0.013 mmol) and **L6b** (74 mg, 0.40 mmol) in 0.5 mL of CDCl₃ were set at $-5\text{ }^{\circ}\text{C}$. The ^1H NMR integrations were measured at intervals of 30 s. The disappearance of (COD)Pd(Me)Cl with time follows first-order kinetics. Treat-

ments of linear regression for $\ln[(\text{COD})\text{Pd}(\text{Me})\text{Cl}]$ versus time afford the evaluation of pseudo-first-order rate constants, k_{obsd} . The second-order rate constants k at various temperatures could be determined according to the rate law of $k_{\text{obsd}} = k[\text{L}]$. The plots of Eyring relationship, $\ln(k/T) = -\Delta H^{\ddagger}/RT + \ln(k_B/h) + \Delta S^{\ddagger}/R$, provide an evaluation of enthalpies and entropies of activation.¹⁰ For the isomerization reactions, the disappearance of the *cis* isomer and the formation of the *trans* isomer, monitored by the ^1H NMR, give consistent first-order rate constants.

Acknowledgment. We thank the National Science Council, Taiwan, ROC, and the NSC-NWO joint project for the financial support.

Supporting Information Available: Kinetics data of geometric isomerism; crystallographic data of **6d**, **6e**, **7d**, and **8a** in CIF format; ORTEP drawings of **6d** and **8a**; and the characterization and synthetic procedure of the new compounds. This material is available free of charge via the Internet at <http://pubs.acs.org>.

(10) (a) Eyring, H. *J. Chem. Phys.* **1935**, *3*, 107. (b) Laidler, K. J.; King, M. C. *J. Phys. Chem.* **1983**, *87*, 2657–2664. (c) Lente, G.; Fabian, I.; Poe, A. J. *New J. Chem.* **2005**, *29*, 759–760.